The intensity detection of single-photon detectors based on photon counting probability density statistics*

Zijing Zhang(张子静)[1,†], Long Wu(吴龙)[2], Jie Song(宋杰)[1,‡], and Yuan Zhao(赵远)[1]

[1] *Department of Physics, Harbin Institute of Technology, Harbin* 150001, *China*
[2] *School of Informatics, Zhejiang Sci-Tech University, Hangzhou* 310018, *China*

(Received 11 February 2017; revised manuscript received 17 May 2017; published online 20 August 2017)

Single-photon detectors possess the ultra-high sensitivity, but they cannot directly respond to signal intensity. Conventional methods adopt sampling gates with fixed width and count the triggered number of sampling gates, which is capable of obtaining photon counting probability to estimate the echo signal intensity. In this paper, we not only count the number of triggered sampling gates, but also record the triggered time position of photon counting pulses. The photon counting probability density distribution is obtained through the statistics of a series of the triggered time positions. Then Minimum Variance Unbiased Estimation (MVUE) method is used to estimate the echo signal intensity. Compared with conventional methods, this method can improve the estimation accuracy of echo signal intensity due to the acquisition of more detected information. Finally, a proof-of-principle laboratory system is established. The estimation accuracy of echo signal intensity is discussed and a high accuracy intensity image is acquired under low-light level environments.

Keywords: single photon detector, photon counting, low light level

PACS: 42.68.Wt, 42.79.Qx **DOI:** 10.1088/1674-1056/26/10/104207

1. Introduction

Single photon detectors have many advantages, such as the single photon sensitivity and extremely high timing precision.[1–4] Single photon detectors have been widely used in many weak signal detection fields, such as remote sensing, biological imaging through highly scattering and absorbing tissues, weak fluorescence imaging, and so on.[5–11] One of the leading applications is remote ranging and imaging with high accuracy. A Geiger mode Avalanche Photodiode Detector (Gm-APD), as one of the single photon detectors, was applied in a lidar system for the first time by MIT Lincoln Laboratories in the JIGSAW project.[12,13] Subsequently, Buller *et al*. used a series of improved techniques based on TCSPC (Time Correlated Single Photon Counting) techniques to demonstrate highly accurate remote detection.[5,7,14,15] Yan *et al.* improved the TCSPC technique-based TOF ranging system, employing pulsed lasers at 1550 nm with multiple repetition rates to offer a robust and convenient method to decrease the range ambiguity.[16] Li *et al.* used the 1.5-GHz sine-wave gated Geiger mode to improve the ranging accuracy of a photon-counting chirped amplitude modulation (CAM) Lidar.[17] Remote ranging and imaging with high accuracy has been implemented by Korean[18] and Chinese groups.[19]

However, Gm-APD has a drawback that the intensity information of the signal is lost. Bao *et al*. used photon number resolving (PNR) detectors and recognized two remote targets with different reflection coefficients at the few-photon level.[20] Liang *et al*. researched a high-speed photon-number resolving detector based on a sinusoidally gated multi-pixel photon counter, which could identify the photon at an average of 7.22 photons/pulse with a repetition frequency of 50 MHz before saturation at room temperature.[21] Besides, Diagne *et al*. used the average firing rate of pixels to obtain the pixel brightness. With a human hand in front of the diffused target illuminated by a 2-μm wavelength pulse signal, an intensity image was acquired using a 32×32 Sb-based Gm-APD array.[22] He *et al*. used the number of triggered pulses within the duration of the pixel dwell time to obtain the optical signal intensity and achieved the passive optical imaging with ultimate sensitivity.[23] Liu *et al*. used the response possibility estimation of laser echo to acquire the intensity.[24] Aongus *et al*. obtained intensity images of a target by calculating the number of detected echo photons in the histogram peak for each individual pixel.[25] Researchers were trying to resolve the loss of the intensity information with single-photon detectors. These existing methods using the photon counting probability of single-photon detectors to gain the intensity information are called the Photon Counting Probability Statistic

*Projiect supported by the Fundamental Research Funds for the Central Universities, China (Grant No. AUGA5710056414), the Program for Innovation Research of Science in Harbin Institute of Technology (Grant Nos. PIRS OF HIT A201412 and PIRS OF HIT Q201505), the National Natural Science Foundation of China (Grant No. 11675046), the Doctoral Fund of the Ministry of Education of China (Grant No. 20122302120003), the Natural Science Foundation of Heilongjiang Province of China (Grant No. A201303), and the Postdoctoral Scientific Research Developmental Fund of Heilongjiang Province, China (Grant No. LBH-Q15060).

†Corresponding author. E-mail: zhangzijing@hit.edu.cn
‡Corresponding author. E-mail: jiesong2002@gmail.com

© 2017 Chinese Physical Society and IOP Publishing Ltd

(PCPS) method.

In this paper, an alternative technique called the Photon Counting Probability Density Statistic (PCPDS) method is proposed. This new method not only counts the triggered number of sampling gates, but also records the triggered time position of photon counting pulses. According to a series of triggered time positions, the photon counting probability density is obtained and used to estimate the echo signal intensity. This new method is capable of improving the estimation accuracy of signal intensity, compared with the existing PCPS method. The rest of this paper is arranged as follows. We first describe the conventional PCPS method and the new proposed PCPDS method. Then, a proof-of-principle laboratory system using Gm-APD is established, and the relative intensity accuracy is compared and analyzed. Finally, a high precision intensity image is acquired under the condition of a few photons per nanosecond.

2. The method description

2.1. The conventional PCPS method

The continuous laser is used to illuminate the target. The fixed width sampling gates are used through controlling the bias voltage of Gm-APD, as shown in the left of Fig. 1(a). The time width of sampling gates is T_g and the time interval of sampling gates is τ_i. The high voltage level in the sampling gates can make Gm-APD work under the Geiger mode. T_g is less than the dead-time, and the number of the triggers in each sampling gate are not more than 1. After every T_g with a high voltage level, there is a τ_i with low voltage level that resets the Gm-APD for the next sampling gate. As long as τ_i is not less than the dead-time τ_d, the detections in all sampling gates will not be affected by the dead time.

Accumulating the detection results of N sampling gates, in which sampling gates are triggered, the photon counting probability will be obtained, as shown in the right of Fig. 1(a). Furthermore, the photon counting probability (the triggered probability of the Gm-APD) can be well described as the Poisson probability function[26] $P = 1 - \exp(-N_s T_g)$ theoretically. Thus, the intensity N_s (usually represented by the mean number of signal photoelectrons per nanosecond) can be estimated with the photon counting probability that is obtained by the detection results of N sampling gates.[27] This method is called the Photon Counting Probability Statistic (PCPS) method in this paper.

2.2. The proposed PCPDS method

In this paper, high precision timing Gm-APD is used not only to count photon counting pulses triggered in sampling gates, but also to record the time positions T_1, T_2, …, T_i, …, T_N of every photon counting pulse in the corresponding sampling gate, shown as the left of Fig. 1(b). T_i is the time position of photon counting pulse in the i-th sampling gate, and T_i starts at the forefront of the sampling gate and stops at the photon counting pulse in the i-th sampling gate. If there is not a photon counting pulse in the i-th sampling gate, T_i does not record any data. Through sampling gates, $\{T_1, T_2, \ldots, T_i, \ldots, T_N\}$ will have valid pulses. According to the recorded $\{T_1, T_2, \ldots, T_i, \ldots, T_N\}$, the photon counting probability density distribution can be obtained as shown in the right of Fig. 1(b). Then, with the Minimum Variance Unbiased Estimation (MVUE) method, the photon counting probability density is used to estimate the echo signal intensity, called the Photon Counting Probability Density Statistic (PCPDS) method in this paper.

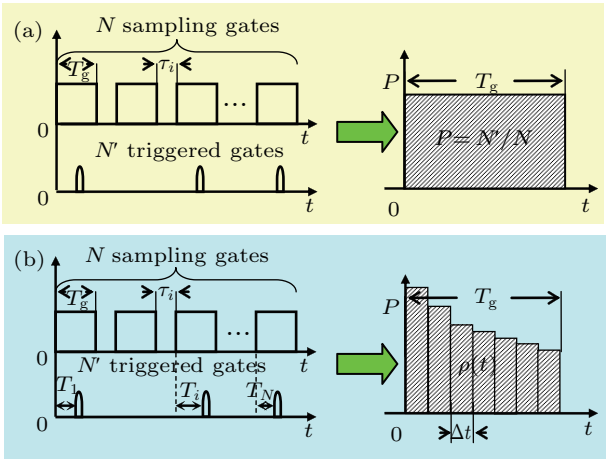


Fig. 1. (color online) (a) Photon counting probability statistics for the conventional PCPS method. (b) Photon counting probability density statistics for the proposed PCPDS method.

The time width of sampling gates T_g is divided into l statistical segments, and the time width of each statistical segment is $\Delta t = T_g/l$. The number of photon counting pulses in the i-th statistical segment is counted, expressed as $N(i)$. The statistical segment is very short, generally on the order of sub nanosecond. Therefore, the practical photon counting probability density in the i-th statistical segment can be expressed as

$$\rho(t) = \frac{\sum_{m=1}^{i}[N(m)/N] - \sum_{m=1}^{i-1}[N(m)/N]}{\Delta t} = \frac{N(i)}{N\Delta t}. \quad (1)$$

In addition, using the Poisson photon counting probability function to take a derivative with respect to the time, we obtain the photon counting probability density theoretically:

$$\rho\,(t)_{\text{theory}} = \frac{\mathrm{d}}{\mathrm{d}t}[1 - \exp(-N_s t)] = N_s \exp(-N_s t). \quad (2)$$

The variance of the photon counting probability density between practical detections and theoretical results, between Eq. (1) and Eq. (2), is

$$\delta^2(N_s) = \sum_{i=1}^{i=l}\left[N_s \exp(-N_s t) - \frac{N(i)}{N\Delta t}\right]^2\Bigg|_{t=i\Delta t}. \quad (3)$$

According to the principle of the minimum variance unbiased estimation, N_s is the minimum variance unbiased estimation if and only if $\delta^2(N_s)$ has the minimum value. Therefore, $\delta^2(N_s)$ is used to take a derivative with respect to N_s and make the derivative zero

$$\frac{\partial}{\partial N_s}\delta^2(N_s) = \sum_{i=1}^{i=l}\left[N_s \exp(-N_s i\Delta t) - \frac{N(i)}{N\Delta t}\right] \times [\exp(-N_s i\Delta t) - iN_s\Delta t \exp(-N_s i\Delta t)] = 0. \quad (4)$$

After the detection of N sampling gates, photon counting distribution $N(i)$ is obtained through the statistics of detection results. At this moment, there is only one unknown parameter N_s in Eq. (4). Using the numerical method, the minimum variance unbiased estimation value of N_s can be obtained through Eq. (4).

3. The experiment and result analysis

In order to characterize the performance of the proposed method in this paper, a proof-of-principle system is established in the laboratory, as shown in Fig. 2. A 532-nm semiconductor continuous laser, whose output power can be adjustable from 0 W to 2 W according to the external driving voltage, in order to simulate different signal intensities. Two galvanometer mirrors are used to control high precision scanning, and the angle range is $\pm 10^\circ$ and accuracy is $\pm 0.01^\circ$. The echo signal is received by the Gm-APD module which consists of a narrow-band filter (the center wavelength is 532 nm, the band width is 8 nm, and the center transmittance is 65%), optical lenses (used to gather the echo signal photons to the photosensitive surface of Gm-APD, and the effective aperture is 25 mm), and a Gm-APD (LASER COMPONENTS COUNT-50C; the photon detection efficiency at 532 nm is 60% approximately; the dead time of the Gm-APD is 50 ns; the timing jitter is 100 ps). The control signal of unified equidistant sampling gates is generated by the signal generator (Tektronix AFG3252), and this control signal is divided into two channels: one channel is used to control the Gm-APD sampling detection and the other channel as the starting signal is transmitted to an oscilloscope. The leading edge of each sampling gate starts timing, and the avalanche pulse of Gm-APD ends timing. A Tektronix DPO4032 oscilloscope is used to record a series of triggers. Finally, all data are collected to the computer for data processing.

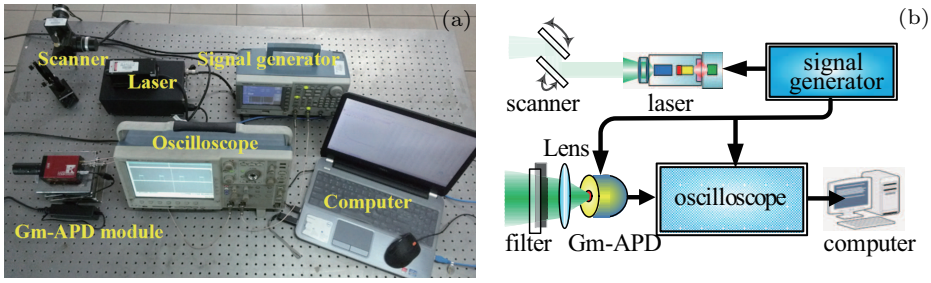


Fig. 2. (color online) (a) Photo of the laboratory system for the proof-of-principle experiment. (b) Experimental setup sketch.

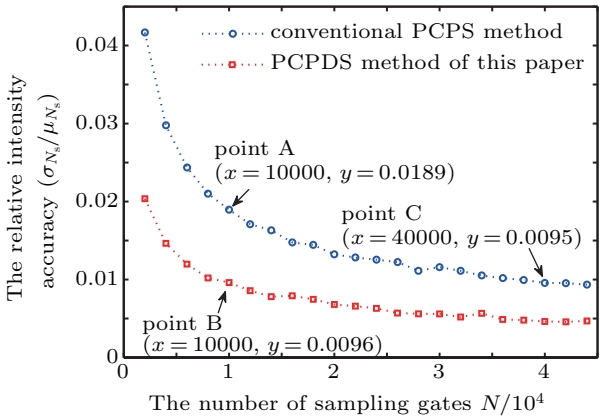


Fig. 3. (color online) The relative intensity accuracy comparison between the proposed PCPDS method and the conventional PCPS method with the number of sampling gates N from 2×10^3 to 4.4×10^3 (circle marks are for the conventional PCPS method and square marks are for the PCPDS method).

The parameters of the system are as follows: the time width of sampling gates is set as $T_g = 4$ ns, and the interval of sampling gates is set as $\tau_i = 96$ ns (it is longer than the dead time of $\tau_d = 50$ ns, in order to be sure of the effectiveness of each sampling gate). The statistical segment width is set as $\Delta t = 100$ ps. In this paper, the relative intensity accuracy is obtained by 100 repeated experiments, and the relative intensity accuracy is defined as the ratio of the standard deviation σ_N to the mean value μ_N, namely σ_N/μ_N.

First, the photon counting probability density statistics (PCPDS) method proposed in this paper and the conventional photon counting probability statistics (PCPS) method are compared with the number of sampling gates N from 2×10^3 to 4.4×10^3. The relative intensity accuracy of two methods are improved with the increase of the number of sampling gates N. However, under the same conditions, the relative intensity accuracy of the PCPDS method of this paper is superior to that of the conventional PCPS method. For example, when 1.0×10^4 sampling gates are employed in both methods, the conventional PCPS method can achieve the relative intensity accuracy of 1.89% (see point A), and the PCPDS method

of this paper can improve the relative intensity accuracy to 0.96% (see point B). If the demand is that the relative intensity accuracy must be less than 1%, the conventional PCPS method needs accumulating about 4×10^4 sampling gates (see point C), while the PCPDS method only needs about 1.0×10^4 sampling gates(see point B). This experimental result demonstrates that the PCPDS method of this paper using the photon counting probability density distribution is better than the conventional PCPS method.

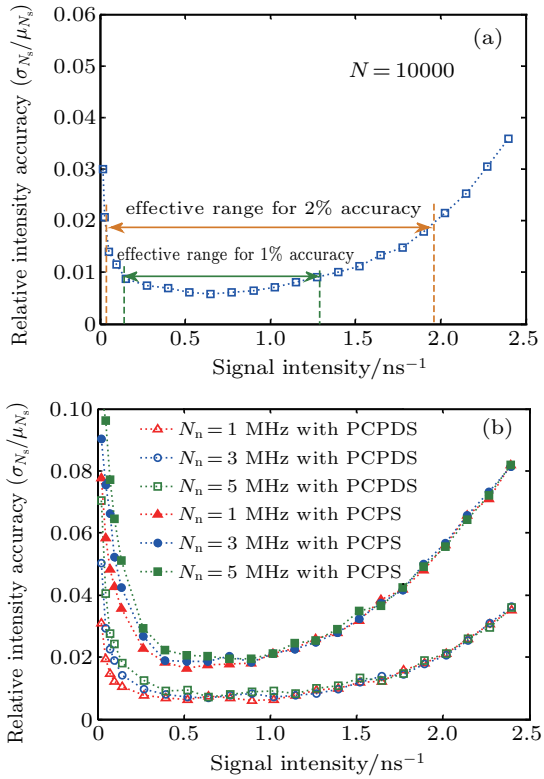


Fig. 4. (color online) (a) The relative intensity accuracy with different signal intensities N_s from 0 to 2.4 ns^{-1} with $N_n = 1$ MHz. (b) The relative intensity accuracy with different noise intensities $N_n = 1$ MHz, $N_n = 3$ MHz, and $N_n = 5$ MHz.

The relative intensity accuracies with different intensities of the echo signal are shown in Fig. 4(a). It is clear that the relative intensity accuracy of the PCPDS method can meet the certain accuracy requirement in a specific range, which is called the effective range. When the signal intensity is stronger than the effective range, Gm-APD tends to be saturated. All sampling gates are almost triggered as soon as the sampling gates just open, and the photon counting probability density becomes insensitive to the change of the signal intensity. Therefore, the relative intensity accuracy becomes worse. When the signal intensity is weaker than the effective range, the effect of noise becomes significant, and thus the relative intensity accuracy becomes worse. For example, considering the accuracy requirement of 1%, the effective range is approximately from 0.15 ns^{-1} to 1.3 ns^{-1} (corresponding to the count rate of from 4.51 MHz to 9.94 MHz); considering the accuracy requirement of 2%, the effective range is approximately from 0.05 ns^{-1} to 1.9 ns^{-1} (corresponding to the count rate of from 1.81 MHz to 9.99 MHz).

Figure 4(b) shows the relative intensity accuracies with different noise intensities of $N_n = 1$ MHz, $N_n = 3$ MHz, and $N_n = 5$ MHz, respectively. In the experiment, a daylight lamp is used to simulate the different noise intensities and illuminate the target. The sun background noise intensity for our experiment system is approximately 1 MHz during a sunny day (it is measured as the number of Gm-APD triggered by noises per second with no signal). In Fig. 4, it can be seen that the relative intensity accuracy becomes worse with the increase of the noise intensity. Besides, the smaller the signal intensity is, the more remarkable the influence of the noise intensity is. This is because the noise intensity becomes the main influence factor when the signal intensity reduces to a certain degree. Therefore, noise reduction is especially important in weak signal intensity detection. Besides, under the condition of the equivalent noise, the PCPDS method of this paper shows an overall improvement compared with the conventional PCPS method.

When the intensity of the echo signal is not in the effective range, a measured intensity value is also obtained, only with no satisfaction of the accuracy. This case will only add an adjustment measurement for satisfying the accuracy requirement. We will use the signal intensity adjustment of a known ratio K to transform the intensity of the echo signal into the effective range. Thus, the measured intensity value after adjustment will be in the effective range and the accuracy requirement is also satisfied. Through this intensity measured value divided by the known adjustment ratio K, the intensity beyond the effective range can be measured satisfying the accuracy requirement.

Finally, the imaging experiment is performed in the laboratory, using the PCPDS method proposed in this paper. As shown in Fig. 5, the imaged target is a piece of white paperboard with three letters H, I, and T with different reflectivities with $\rho_H < \rho_I < \rho_T$.

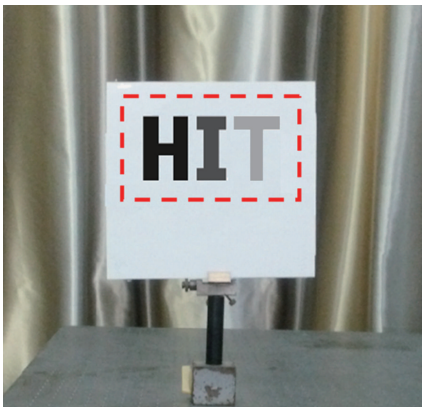


Fig. 5. (color online) Photograph of the imaged target. The dashed box is the detection area.

Figures 6(a) and 6(b) are the imaging results and the corresponding intensity data statistics with the conventional

PCPS method. Figures 6(c) and 6(d) are the imaging results and the corresponding intensity data statistics with our PCPDS method. In Fig. 6, different colors represent different intensities of echo signals from 0.3 ns^{-1} to 2 ns^{-1}. Comparing Figs. 6(a) and 6(c) directly, the PCPDS method of this paper obtains a better image with small fluctuations in the image. Then the intensity data statistical results of two methods are compared. At the edge of three letter targets, the laser spot may cover both the target and background plate, therefore causing great errors. Intensity data statistics in Figs. 6(b) and 6(d) have got rid of the edge data. Figure 6(b) shows statistical results of the conventional PCPS method, the mean intensities of three letters H, I, and T are 0.4103, 0.7723, and 1.2094 and the standard deviations are 0.0081, 0.0135, and 0.0258, respectively. Thus, the relative intensity accuracy for three letters (H, I, and T) can be obtained as 1.97%, 1.75%, and 2.13%, respectively. While figure 6(d) shows statistical results of the PCPDS method of this paper, the mean intensities of three letters H, I, and T are 0.4011, 0.7677, and 1.2166 and the standard deviations are 0.0034, 0.0051, and 0.0116, respectively. Thus, the relative intensity accuracy for three letters (H, I, and T) can be obtained as 0.85%, 0.67%, and 0.95%, respectively. It is clear that the PCPDS method of this paper improves the relative intensity accuracy efficiently, compared with the conventional PCPS method.

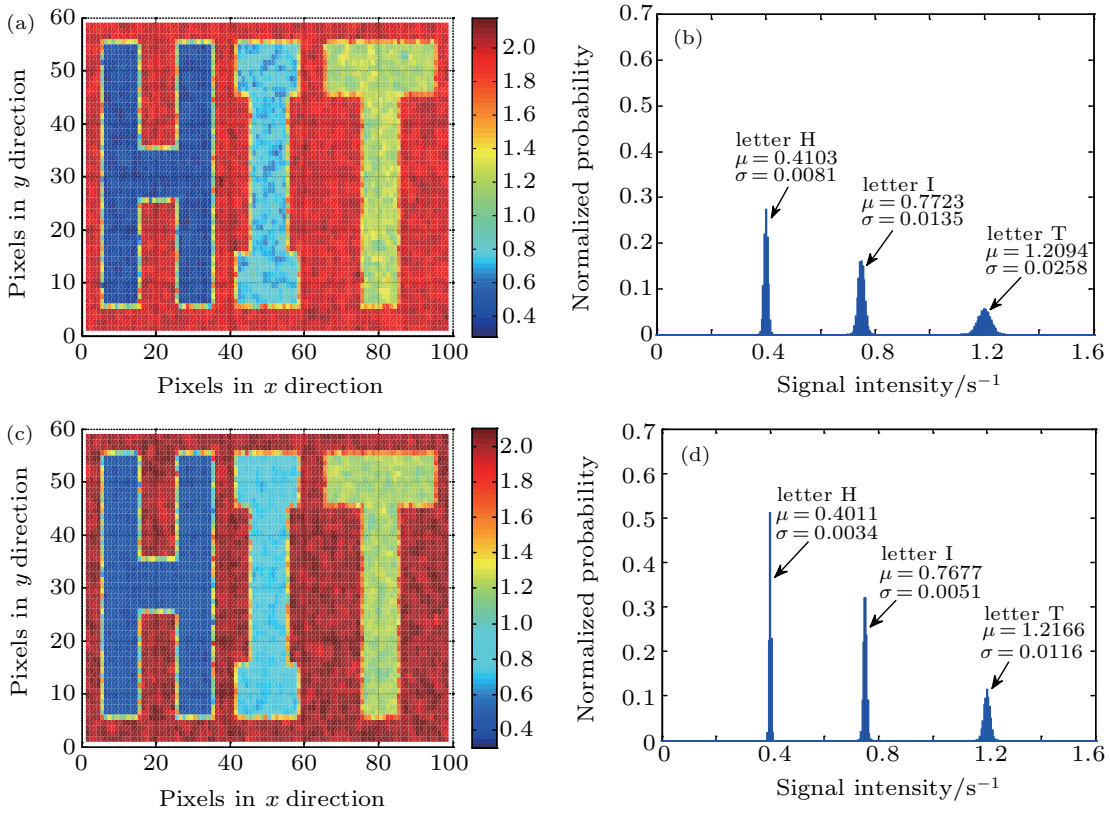


Fig. 6. (color online) The imaging results and analysis. (a) The imaging results 60×100 pixels with the conventional PCPS method. (b) Intensity data statistics for letters H, I, and T in panel (a). (c) The imaging results 60×100 pixels with the PCPDS method proposed in this paper. (d) Intensity data statistics for letters H, I, and T in panel (c).

4. Conclusion and perspectives

In this paper, a PCPDS method for retrieving the ultra-weak signal intensity based on single-photon detectors has been demonstrated. This method uses photon counting probability density statistics to estimate the signal intensity, which improves the estimation accuracy of signal intensity compared with the conventional PCPS method. A proof-of-principle laboratory system is established, and the relative intensity accuracy is analyzed. There is an effective range of signal intensity for a certain accuracy requirement, and the intensity estimation accuracy becomes worse with the intensity out of the effective range. Finally, a high accuracy intensity image is acquired under low-light level environments successfully.

References

[1] Rosenberg D, Kerman A J, Molnar R J and Dauler E A 2013 *Opt. Express* **21** 1440
[2] Marsili F, Verma V B, Stern J A, Harrington S, Lita A E, Gerrits T, Vayshenker I, Baek B, Shaw M D, Mirin R P and Nam S W 2013 *Nat. Photon.* **7** 210
[3] Yuan Z L, Sharpe A W, Dynes J F, Dixon A R and Shields A J 2010 *Appl. Phys. Lett.* **96** 071101
[4] Liu J, Zhang L Q, Jiang Z N, Ahmad K, Liu J S, and Chen W 2016 *Chin. Phys. Lett.* **33** 088502
[5] Krichel N J, McCarthy A and Buller G S 2010 *Opt. Express* **18** 9192
[6] Lee J, Kim Y J, Lee K, Lee S and Kim S W 2010 *Nat. Photon.* **4** 716

[7] Hiskett P A, Parry C S, McCarthy A and Buller G S 2008 *Opt. Express* **16** 13685

[8] Kirmani A, Venkatraman D, Shin D, Cola?o A, Wong F N, Shapiro J H and Goyal V K 2014 *Science* **343** 6166

[9] Li W, Hu H and Dutta N K 2013 *J. Mod. Opt.* **60** 1741

[10] Liang Y, Wu E, Chen X, Ren M, Jian Y, Wu G and Zeng H 2011 *IEEE Photon. Technol. Lett.* **23** 887

[11] He Y H, Lv C L, Zhang W J, Zhang L, Wu J J, Chen S J, You L X and Wang Z 2015 *Chin. Phys. B* **24** 060303

[12] Marino R M, Stephens T, Hatch R E, McLaughlin J L, Mooney J G, O'Brien M E, Rowe G S, Adams J S, Skelly L, Knowlton R C, Forman S E and Davis W R 2003 *Proc. SPIE* **5086** 1

[13] Marino R M and Davis W R 2005 Jigsaw: a foliage-penetrating 3D imaging laser radar system, *Lincoln Lab. J.* **15** 23

[14] Hao J, Gong M, Du P, Lu B, Zhang F, Zhang H, and Fu X 2016 *Chin. Phys. B* **25** 074207

[15] McCarthy A, Collins R J, Krichel N J, Fernandez V, Wallace A M and Buller G S 2009 *Appl. Opt.* **48** 6241

[16] Liang Y, Huang J, Ren M, Feng B, Chen X, Wu E, Wu G and Zeng H 2014 *Opt. Express* **22** 4662

[17] Li Z, Bao Z, Shi Y, Feng B, Wu E, Wu G and Zeng H 2015 *IEEE Photon. Technol. Lett.* **27** 616

[18] Oh M S, Kong H J, Kim T H, Jo S E, Kim B W and Park D J 2011 *J. Opt. Soc. Am. A* **28** 759

[19] Ren M, Gu X, Liang Y, Kong W, Wu E, Wu G and Zeng H 2011 *Opt. Express* **19** 13497

[20] Bao Z, Liang Y, Wang Z, Li Z, Wu E, Wu G and Zeng H 2014 *Appl. Opt.* **53** 3908

[21] Liang Y, Ren M, Wu E, Wang J, Wu G and Zeng H 2012 *IEEE Photon. Technol. Lett.* **24** 1852

[22] Diagne M A, Greszik M, Duerr E K, Zayhowski J J, Manfra M J, Bailey R J, Donnelly J P and Turner G W 2011 *Opt. Express* **19** 4210

[23] He W J, Chen Y J, Chen Q N, Gu G H and Cheng W 2012 *Proc. SPIE* **8366** 83660T

[24] Liu H, Yin W Y, Miao Z, He W J, Chen Q and Gu G H 2013 *Proc. SPIE* **9045** 904507

[25] McCarthy A, Krichel N J, Gemmell N R, Ren X, Tanner M G, Dorenbos S N, Zwiller V, Hadfield R H and Buller G S 2013 *Opt. Express* **21** 8904

[26] Johnson S, Gatt P and Nichols T 2003 *Proc. SPIE* **5086** 359

[27] Wang F 2013 *Proc. SPIE* **8905** 89050I